

# Coexistence of coil and globule domains within a single confined DNA chain

Baeckkyoung Sung, Amélie Leforestier and Françoise Livolant\*

Laboratoire de Physique des Solides, CNRS, Univ Paris-Sud, Université Paris-Saclay, 91405 Orsay Cedex, France

Received October 12, 2015; Revised December 8, 2015; Accepted December 9, 2015

## ABSTRACT

**The highly charged DNA chain may be either in an extended conformation, the coil, or condensed into a highly dense and ordered structure, the toroid. The transition, also called collapse of the chain, can be triggered in different ways, for example by changing the ionic conditions of the solution. We observe individual DNA molecules one by one, kept separated and confined inside a protein shell (the envelope of a bacterial virus, 80 nm in diameter). For subcritical concentrations of spermine (4+), part of the DNA is condensed and organized in a toroid and the other part of the chain remains uncondensed around. Two states coexist along the same DNA chain. These ‘hairy’ globules are imaged by cryo-electron microscopy. We describe the global conformation of the chain and the local ordering of DNA segments inside the toroid.**

## INTRODUCTION

The DNA molecule is a semiflexible and highly charged polyelectrolyte that exists in a coil conformation in ‘good solvent’ conditions. The molecule can be collapsed into a globule by numerous agents (1): the addition of alcohol that changes the quality of the solvent (80% alcohol in water is commonly used), the addition of neutral crowding agents such as PolyEthylene Glycol (PEG) through an excluded volume mechanism or the addition of multivalent cations (spermine, spermidine, cobalt hexamine (CoHex), cationic polypeptides and basic proteins). As for other stiff polymers, the transition is predicted to be first order (2,3) and two distinct states have been detected experimentally for example by a large and discontinuous reduction of the radius of gyration in light scattering experiments performed for a population of chains in bulk conditions (4).

The morphology of the DNA condensed particles has drawn much interest especially after the first electron microscopy observation of the DNA globules (5,6) showing the frequent toroidal conformation of DNA, although

spheres and rods were found sometimes (7). This interest has been renewed in the last years with the hope to be able to control the size and charge of the genetic material for potential gene delivery applications. Nevertheless, classical electron microscopy methods that require to dehydrate the sample and to add contrasting agents ruled out high resolution studies. These limitations can be overcome by cryo-electron microscopy (cryoEM) that keeps unchanged the water and ionic environments of the molecule. Hud and Downing (8) revealed how this method is powerful and well suited to analyze details of the DNA chain conformation. In spite of this work, the systematic analysis of the globular DNA conformations encounters other limitations. The collapse transition of individual chains must be separated from the aggregation that involves several chains. Widom and Baldwin (9) were able to get rid of the aggregation effect by using CoHex as the condensing agent and by working at very low concentrations of  $\lambda$ -DNA (below 0.2  $\mu\text{g/ml}$ ). However, when spermine and spermidine were used as condensing agents, it has not been possible to separate the collapse from the aggregation in conditions that were successful for CoHex (9). Jary and Sikorav were able to analyze the coil-globule transition before aggregation starts, by working at shorter times with extremely low concentrations of DNA (50 ng/ml) (10,11). Nevertheless, such experimental constraints prevent any systematic structural analysis of the DNA chain conformation by cryoEM.

Very little was thus known about the conformation of individual DNA chains at the coil-globule transition until the development of high sensitivity methods of fluorescence microscopy (12) that made possible the observation of individual chains. Ueda *et al.* (13) found that an individual T4 DNA chain (166 kbp) confined between slide and coverslip exhibits a first order transition between an elongated coil and a compact globule with a change in the concentration of alcohol added to the aqueous solution. Interestingly, they observed a metastable state in the globular phase near the transition point in which the globular and coil states coexist within a single DNA chain in a way somewhat similar to what has been observed in other systems (14,15).

We described earlier a method to perform cryoEM observations of individual DNA chains at a reasonable DNA

\*To whom correspondence should be addressed. Tel: +33 1 69 15 53 92; Fax: +33 1 69 15 60 86; Email: francoise.livolant@u-psud.fr  
Present address: Baeckkyoung Sung, Centre de Recherche Paul Pascal (CNRS UPR8641), 115 av Schweitzer, 33600 Pessac, France.

concentration and without aggregation (16,17). We use the bacteriophage T5 and trigger its DNA ejection *in vitro* upon interaction of the phage with its receptor FhuA. The ejection can be stopped before the ejection is complete. Fragments of the chains, whose length ranges from a few hundreds of base pairs to the full genome (121 000 bp) are thus kept in each capsid (80 nm in diameter) and cannot interact with each other. The capsid being permeable to water and ions, each chain is entrapped in its own dialysis bag and ionic conditions can be reversibly modified. The conformation of the DNA chain changes accordingly. Using this method, we analyzed previously the conformation of the chain under 'good solvent' conditions, in the absence of any condensing agent (the chain occupies the whole capsid) (17) and after it is collapsed into a toroidal globule by 5 mM spermine (16). The aim of the present paper is to monitor the changes of the conformation of individual double stranded DNA macromolecules at the collapse transition. We have tested several concentrations of the tetravalent cation spermine and we also varied the concentration of the added monovalent salt concentration (NaCl). We evidence a variety of conformations ranging from pure toroids of decreasing densities to complex conformations that raise new questions on the underlying mechanisms of DNA collapse. These conformational states of the molecule may be also relevant for biological regulation of DNA functional properties inside the living cell.

## MATERIALS AND METHODS

T5 wt bacteriophages were produced in *Escherichia coli* Fsu $\beta$ + and purified as described by Bonhivers *et al.* (18). They were suspended at a concentration of  $1 \times 10^{13}$  phages/ml in 10 mM Tris pH7.6, 1 mM MgCl<sub>2</sub>, 1 mM CaCl<sub>2</sub>. The protein receptor FhuA was purified as described earlier (18) and stored in 250 mM NaCl, 1% (w:v) octyl glucoside and 10mM Tris, pH 8, at a concentration of 2.6 mg/ml. During the experiments, the detergent concentration was kept constant at all steps of the procedures (either octyl glucoside (OG) 1% or lauryldimethyl-amine N-oxide (LDAO) 0.03%).

### Partial ejection and condensation of the DNA chain inside the capsid

The preparation of the samples is sketched in Figure 1. A concentrated solution of T5 bacteriophages is maintained at 4°C in the presence of the receptor FhuA at a final T5:FhuA ratio of 1:500, with 15% PEG 6000 (to apply an external osmotic pressure of 3.2 Atm that blocks the ejection at intermediate steps, see (19)) and DNase (Amersham Bioscience, 5 units/ $\mu$ l) to digest the ejected DNA. After 4 h at 37°C, most phages have ejected a fraction of their DNA. Each capsid contains a unique DNA fragment. A negligible volume of spermine solution is then added. Spermine diffuses through the protein capsid and initiates the conformation change of the DNA chain in the capsid. The sample is then diluted 4 times to dilute PEG without changing the spermine and ionic concentrations and equilibrated for 1 h to a few days at 4°C before preparation of thin vitrified films.

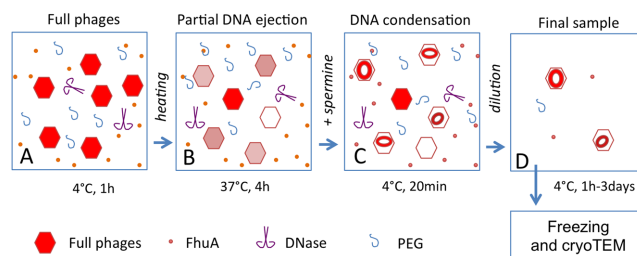


**Figure 1.** Schematic drawing of the experimental protocol. (A) The sample contains full T5 bacteriophages, FhuA receptor, PEG 6000 and DNase but ejection is hindered at low temperature. (B) The heating to 37°C triggers DNA ejection. (C) The addition of spermine condenses DNA fragments remaining inside the capsids. (D) The sample is diluted to reach a non condensing PEG concentration (below 15%) before preparation of thin films for cryoEM observations.

The final concentration of bacteriophages is equal to  $1.1 \times 10^{12}$  phages/ml (0.45 mM DNA Phosphates). In the first set of experiments, we tested three concentrations of spermine (0.05, 0.1 and 0.5 mM) in 10 mM Tris buffer pH 7.6, 7 mM NaCl, 1 mM MgCl<sub>2</sub> and 1 mM CaCl<sub>2</sub>. We reproduced the experiments in the same buffer with  $2.5 \times 10^{12}$  phages/ml and 0.8 mM spermine (1 mM DNA Phosphates). We also analyzed samples prepared in 10 mM Tris buffer pH 7.6, 137 mM NaCl, 0.8 mM MgCl<sub>2</sub>, 0.08 mM CaCl<sub>2</sub> and 5 mM spermine, with a T5 concentration of  $3.2 \times 10^{13}$  phages/ml (13 mM DNA Phosphates).

### Cryoelectron microscopy

A total of 3  $\mu$ l of the solution are deposited on a glow-discharged holey carbon grid (Quantifoil R2/2, Jena, Germany). The grid is blotted with a filter paper for 2–3 s to remove the excess of the solution, and directly plunged into liquid ethane cooled down by liquid nitrogen. During the preparation of the samples, the temperature and relative humidity of the environment are kept at 20–21°C and 89–96%, respectively, in a home-made device. Frozen samples are transferred into a Gatan 626 cryostage (Gatan, Warrendale, USA) and observed in a transmission electron microscope (JEOL-2010 and JEOL-2010F, Japan) operated at 200 kV. All images are recorded on Kodak SO163 negative films under low dose conditions at a magnification of X50000 and 900 or 3000 nm underfocus, to image DNA packing and the overall shape of the objects, respectively. The films are developed in full strength Kodak D19 for 12 min, and scanned with a Nikon Coolscan 9000 at a resolution of 4000 pixels per inch. Quantification of the relative amounts of condensed and uncondensed DNA have been done by looking at capsids on the screen.

## RESULTS

Following the protocol described in Figure 1, we handle a population of capsids, each containing a unique DNA chain. A few bacteriophage capsids are empty. A few remain full and most have ejected part of their DNA content. We first explored a range of low spermine concentrations (0.05, 0.1 and 0.5 mM) in low salt buffer (10 mM Tris, 7mM NaCl, 1 mM MgCl<sub>2</sub>, 1 mM CaCl<sub>2</sub>). There is not enough spermine

to fully neutralize DNA in 0.05 and 0.1 mM spermine, the charge ratio  $R$  (+/−) being respectively equal to 0.44 and 0.88 compared to 4.4 in 0.5 mM spermine.

For  $C_{\text{spermine}} = 0.5$  mM, all incompletely filled capsids present toroids (Figure 2A). They are visible under multiple orientations: side views (capsids 2 and 3), top views (capsid 7) and oblique views (capsid 4). The toroids present the characteristics described earlier (8,16): a hexagonal packing of the DNA segments, a faceting of the bundle section, and the alignment of the reticular planes parallel to the faces of the capsid (enlargements of capsids 3 and 6). The interhelix spacing  $a_H = 2.8 \pm 0.2$  nm is measured on lattices or deduced from the well defined periodic striations with  $d = a_H\sqrt{3}/2$  seen locally under favorable orientations (capsid 6). The length of each DNA fragment trapped in the capsid can be determined when toroids are seen in side views, by measuring the diameter and the section of the toroid—to determine its volume—and the interhelix distance  $a_H$ . As an example, the toroid in capsid 2, is made of a 6  $\mu\text{m}$  long DNA fragment. In most cases, the external diameter of the toroid is fixed by the internal diameter of the capsid (toroids 2, 3, 7). Short DNA chains may form toroids with a diameter smaller than the capsid (toroids 1, 4). Longer chains form distorted toroids, in good agreement with theoretical predictions (20) and previous observations.

For  $C_{\text{spermine}} = 0.1$  mM, we also recognize capsids filled with variable amounts of DNA (Figure 2B and C). The local hexagonal ordering of DNA is still recognized but it is often less defined than in toroids formed at 0.5 mM sp. The DNA lattice shows larger interhelix distances ( $a_H = 3.0 \pm 0.2$  nm). The faceting is not so clearly seen although the main reticular planes are still aligned parallel to the capsid surface (detail of capsid 4 in Figure 2B). Unexpectedly, DNA densities can also be detected in the core of a few top view toroids (Figure 2C, arrows).

For  $C_{\text{spermine}} = 0.05$  mM, we notice a larger range of DNA patterns inside the capsids (Figure 2D). The overall shape of toroidal structures may be recognized sometimes (capsid 1 with a short DNA length and capsid 4 with a larger one) but the DNA segments are loosely packed (enlargement of capsid 4), with larger and more fluctuating interhelix distances ( $a_H = 3.2 \pm 0.6$  nm) and may sometimes not be recognized at all. In other capsids there is no recognizable toroid; DNA looks granular and occupies all the capsid volume (capsid 3). Such disordered structures are better imaged at larger defocus. We thus systematically imaged the samples twice: (i) at low defocus first (900 nm) to access the lattice spacing and to analyze the local DNA order in condensed states (Figure 2) and (ii) with a high defocus value (3000 nm) to enhance the contrast at low spatial frequencies and to visualize the overall shape of the object. Supplementary Figure S1 shows a selection of capsids imaged at these two defocus values for comparison.

We present on Figure 3 a selection of images acquired at large underfocus to highlight differences between DNA conformations observed at 0.5 and 0.05 mM spermine. An empty capsid located nearby the capsid of Figure 3A2 is shown for comparison (Figure 3A1). Intensity profiles have been recorded along the white rectangular frames colored in green for the empty capsid, in red for the toroidal DNA

and in orange for disordered DNA located outside of the toroids. The fluctuations of the intensity signal are low in the vitrified film of water (gray) and in the empty capsid (green) with a very modest difference between the two mean values that corresponds to the signal of the protein capsid wall made of twice one layer of proteins. By comparison, the signal from the toroidal DNA (red) is higher, as well as, to a less extent, the signal from the non-toroidal DNA. Toroids formed at 0.5 mM sp present sharp limits either in top and side views (Figure 3A2 and 3). In contrast, boundaries of the toroids are less defined at 0.05 mM sp (Figure 3B) and the intensity signal shows more fluctuations (Figure 3B1). We also observed a few capsids containing DNA with no toroidal structure (Figure 3B2). In such cases the DNA granularity seems to be coarser than in the absence of spermine (purely DNA–DNA repulsive interactions, (19)). These images let us suspect a continuum of different DNA states inside the capsid, ranging from a fully uncondensed coil to conformations with condensed and uncondensed domains either dispersed in the capsid (grainy capsids) or gathered into a single toroidal domain (hairy toroids) and finally to a single toroid made of the entire DNA chain. We obtained similar intra capsid DNA patterns in an independent series of experiments, using 0.08 mM spermine (see Supplementary Figure S2). We also explored the effect of increasing the concentration of added monovalent salt (NaCl) that is known to lower the spermine attractive interactions between DNA, and observed again similar original DNA conformations (see Supplementary Figure S3).

Thus, for a given range of ionic conditions, we observe the coexistence of two states along the same DNA chain: the condensed (toroidal) DNA and the coiled uncondensed DNA that occupies the remaining free volume around. We may roughly estimate that uncondensed DNA represents about  $44 \pm 29\%$  of the total encapsidated DNA in 0.05 mM spermine and  $12 \pm 8\%$  in 0.1 mM spermine compared to 0% in 0.5 mM spermine (Figure 4). These estimations have been done on a short selection of capsids (78 capsids in 0.5 mM sp, 11 in 0.1 mM sp and 45 in 0.01 mM sp). Many capsids containing a short length of encapsidated DNA were discarded because the signal of uncondensed DNA was not significantly different from the background. Although the dispersion of the values is high, especially at  $C_{\text{spermine}} = 0.05$  mM, we are confident that these estimations provide a significant information.

$a_H$  values measured in the toroids are plotted on the same graph.  $a_H$  decreases from  $3.24 \pm 0.09$  nm at 0.05 mM sp to  $2.99 \pm 0.06$  nm at 0.1 mM sp and to  $2.85 \pm 0.03$  nm at 0.5 mM sp (Figure 4). An analysis of variance reveals that there is a significant difference between the means of the three series of data ( $P < 1.4 \times 10^{-5}$ ). Pairwise comparisons of the means shows that each mean is significantly different from the others ( $P$ -value  $< 0.04$  in the three comparisons). The largest distances are compatible with a cholesteric instead of a hexagonal liquid crystalline organization of DNA in the globule, and agree with the predicted possible coexistence of several globular states of DNA (3).

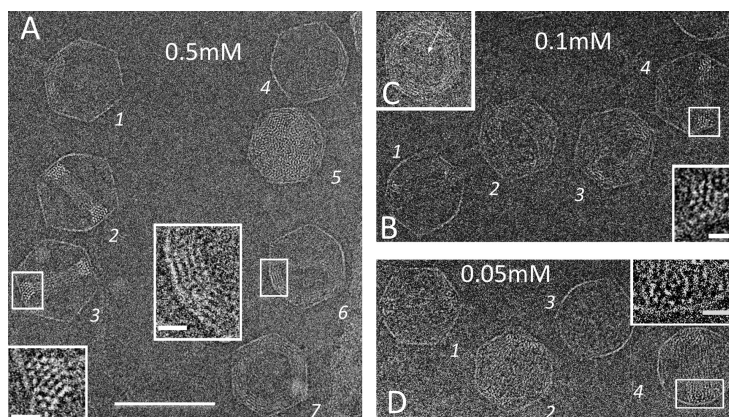


**Figure 2.** CryoEM of DNA condensed inside the T5 bacteriophage capsids for various concentrations of spermine: 0.5 mM (A), 0.1 mM (B and C) and 0.05 mM (D) in the same buffer (10 mM Tris, 1 mM MgCl<sub>2</sub>, 1 mM CaCl<sub>2</sub>, pH 7.6). Details of the DNA packing in the toroids are enlarged (inserts). Images are taken at  $-900$  nm underfocus. Scale bar = 100 nm in the figures and 10 nm in the inserts.

## DISCUSSION

### Domain of coexistence between coils and globules

CryoEM of individual DNA chains trapped in the semi-permeable capsids let us explore the conformation of the individual DNA chain in this coexistence region, between the region of pure coils, in the absence of any condensing agents (19) and the region where all chains are fully collapsed into toroids (0.5 mM sp in this work and 5 mM sp in (16) (Figure 5). The coexistence of coils and globules has been reported long ago by Gosule and Schellman (21) by analyzing flow linear dichroism signals of very dilute T7 DNA solutions to which increasing amounts of the polyamines spermidine and spermine were added under low ionic strength conditions (2 mM monovalent ions). It was also observed by Post and Zimm (4) by light scattering experiments with magnesium in ethanol-water solvent. More recently, Yoshikawa *et al.* observed directly the coexistence of ‘giant’ T4 molecules coils and globules by fluorescence microscopy in highly dilute solutions with a large variety of condensing agents (12–13,22–23). When long DNA chains are condensed by the tetravalent polyamine spermine, the transition region between the two extreme states of pure coils and pure globules is rather narrow compared to the divalent and trivalent polyamines (24). Jary and Sikorav (11) also studied by sedimentation the conformation of Lambda DNA chains. They defined five regions for increasing spermidine (3+) concentrations. In two of them coils and globules coexist, on both sides of the region of pure globules.

### Coexistence of two states along a single DNA chain

We observe a continuum of DNA conformations between the pure coil that occupies the entire volume of the capsid and the fully condensed toroidal globule. In many cases, the single chain forms ‘hairy’ toroids, the chain being partly in a coil and partly in a toroidal conformation. This situation corresponds to an intra-molecular phase separation. These original conformations have been observed when there is a deficit of added positive charges. They have been found also when large amounts of monovalent salts compete with spermine for condensation onto DNA. The coexistence of

coiled and globular domains along a single chain corresponds probably to equilibrium states since they are observed systematically 1 h after addition of spermine and are still present 3 days later. Nevertheless, we cannot exclude that they are metastable states.

One main interest of cryoTEM is to control the ionic environment of the chain and to avoid the presence of dyes that may interfere with DNA electrostatics. CryoTEM also avoids multiple steps of preparation required in classical Transmission Electron Microscopy (TEM). Despite the limitations of classical TEM (adsorption on a positively charged surface, dehydration and addition of charged contrasting agents such as uranyl acetate) a few globules connected to disperse DNA around have been described and suspected to be incompletely formed globules or globules in the process of being unraveled (10). We suspect they correspond to our ‘hairy’ globules.

From the two series of data presented on Figure 4, we calculated the concentration of DNA in the collapsed and in the coiled domains for each spermine concentration. The decrease in concentration, from  $474 \pm 60$  to  $413 \pm 60$  and to  $363 \pm 150$  mg/ml in the toroid correlates with the increase of concentration in the dilute phase, from almost 0 to 9 and to 40 mg/ml. The difference between the DNA concentrations in the two states thus decreases significantly (from 474 to 320 mg/ml) when lowering the spermine concentration (the charge ratio  $R(+/-)$ ). This behavior would probably deserve a deeper analysis, taking into account the influence of the DNA length/concentration on the fraction of condensed/uncondensed DNA. For this, it would be useful to handle a population of capsids containing DNA segments of identical length. Bacteriophages such as Lambda may be considered since they have been shown to eject a DNA segment of a given length for each applied osmotic pressure (25), as opposed to T5 for which the ejection stops at several steps for a given applied pressure (17).

### Average density of the globule

The ratio between the coil and the toroidal DNA fragments, and the interhelix spacing in the toroid determine the average density of the DNA globule. Our observations

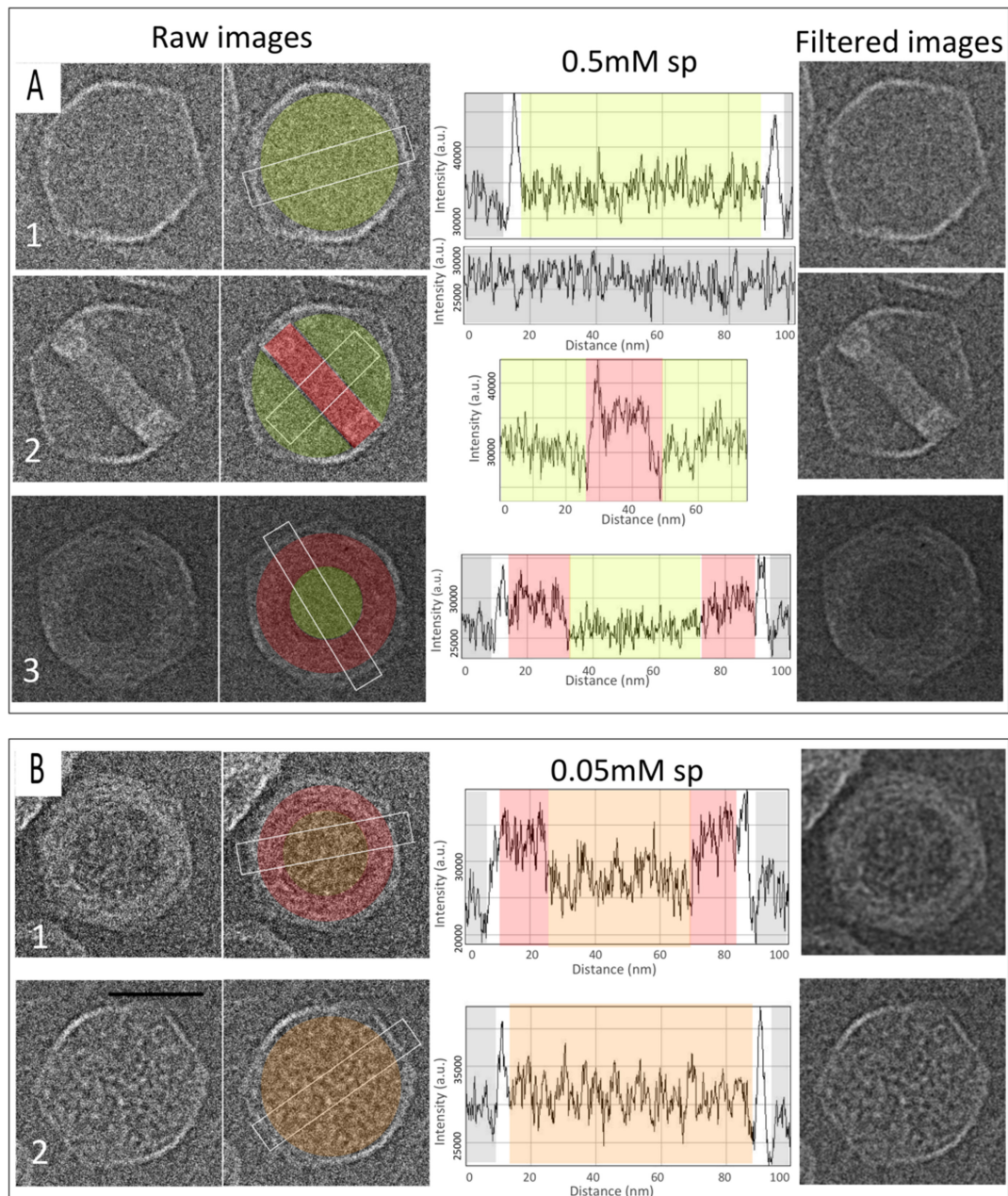


**Figure 3.** Comparison of intensity profiles recorded on raw images for two spermine concentrations: 0.5 mM (A) and 0.05 mM (B). In (A) DNA fully condensed in the toroid (red) distinguishes clearly from the empty part of the capsid (green) and from the vitrified film of water around (grey). In contrast, at lower spermine concentration, part of the DNA is found outside of the toroid (B1) or may even occupy the whole capsid and present a grainy structure (B2) that may be differentiated on the profiles (orange). Images were recorded at  $-3000$  nm defocus, scanned at 4000 dpi and analyzed using ImageJ. The visualization of uncondensed DNA was enhanced on filtered images using wavelet filtration (ImageJ, A trous filter with  $k_1 = 100$ ,  $k_2 = 100$ ,  $k_3 = k_4 = k_5 = 0$ ). Scale bar = 50 nm.

agree with measurements of sedimentation coefficient (Cs) of DNA globules condensed by spermidine in 10 mM Tris buffer at a concentration of 50 ng DNA/ml (10–11). The authors reported the coexistence of globules with Cs = 180S with coils of a much lower density (40S) in the coexistence region. Their density increases up to 380S in the domain where all chains are condensed into globules. The increase from 180S to 380S likely reflects mostly the decrease of the interhelix spacing with the variation of the spermidine

concentration. The visualization of intermediate states of monomolecular condensation reveals that the collapse transition is not a two state reaction, in agreement with measurements of the diffusion coefficient of Lambda chains collapsed by CoHex through the transition zone, in solutions equilibrated for 16 h (9).

The measured decrease of the interhelix distance with the spermine concentration is also consistent with X-ray scattering data collected with short DNA fragments in the high

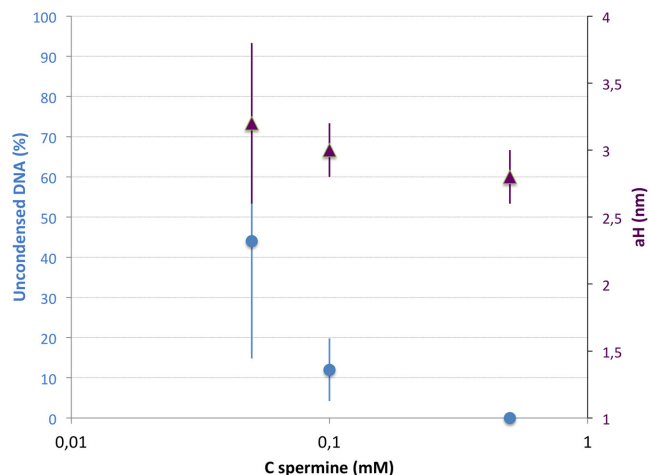


**Figure 4.** Estimations of the percentage of uncondensed DNA (filled circles) and measures of aH values in the toroids for three spermine concentrations (0.05, 0.1 and 0.5 mM) (triangles). Bars represent the dispersions of values around the average, which may be much larger than the estimated error ( $\pm 5\%$ ).

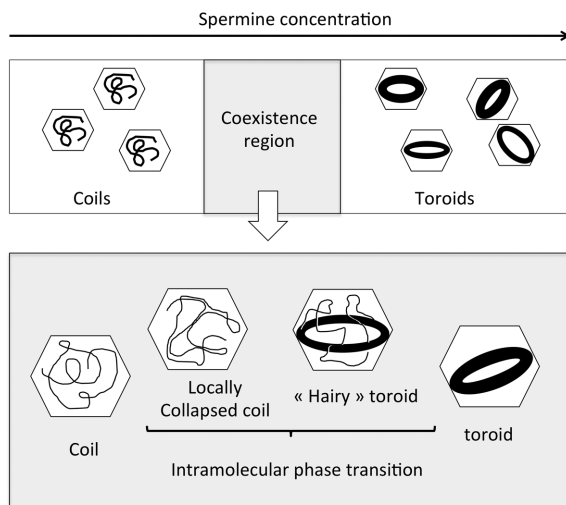


**Figure 5.** Schematic representation of our observations. In the coexistence region, not only pure coils and pure toroidal globule coexist but also intermediate configurations: locally collapsed coils and hairy toroids.

DNA concentration regime (around 90 mM DNA phosphate) (26,27). Starting with Na-DNA, a fraction of DNA is aggregated at spermine concentrations above 15 mM (i.e. 60 mM positive charges) close to the charge compensation and was collected for diffraction experiments. The interhelix distances decreases first until all condensed monovalent counterions are replaced by spermine. In our experiments, DNA was neutralized in the capsid mostly with Na counterions, but divalent ions were also present to maintain the stability of the full capsids at the initial stages of our experiments. We also worked with a larger concentration of added salt (10 mM Tris, 7 mM NaCl, 1 mM MgCl<sub>2</sub>, 1 mM CaCl<sub>2</sub>) compared to 10 mM Tris in Raspaud *et al.*. Our experiments are also performed at lower DNA concentration, 0.45 mM phosphate compared to 90 mM phosphate. This DNA concentration takes into account the to-

tal volume of the sample, with the DNA inside the capsids and also the nucleotides outside of the capsids that result from the nuclease activity. Nevertheless, this concentration seems to be high enough to follow the progressive release of the initially condensed monovalent (and divalent) counterions upon addition of spermine. As reported before, the presence of monovalent counterions initially condensed on DNA controls the interhelix distance (26). The fact that spermine is added directly to the DNA solution whereas it is added here to the buffer does not matter because added spermine cations freely diffuse through the capsid and immediately condense onto DNA.

### Coil-globule transition under 2D or 3D confinement

As explained above, it is difficult to explore the collapse of individual chains in the bulk because of aggregation effects. In most fluorescence experiments, DNA chains are confined in two dimensions, between slide and coverslip, which leads to the 'extended coil' configuration of the chain. Additional stretch may also be introduced, for example under flow (28,29). Under such geometrical constraints, depending on the condensing agents and on the salt conditions, the collapse transition can proceed by one of two ways, either (i) a direct transition from the coil to the globule or (ii) via an intermediate intrachain segregated state (24,11). A few authors (28,30) report the existence of a pearling structure composed of several rings interconnected by elongated coil parts along the chain. Under 3D confinement, we never observed such configurations, but instead a single toroid. Other experiments would be needed to explore more systematically the 3D confinement effect, by monitoring the radius of the sphere and the DNA length. Of course confinement of DNA chains inside small spheres is different from planar or cylindrical confinement because conformational space is unbounded in the 1D and 2D case, but not in 3D confinement, as pointed out in many theoretical works (see for example (31–37)).

### Biological relevance of a complex globular conformation of DNA

In the coexistence region where the complex globule configurations are observed, spermine cations are not in sufficient amount to collapse the total DNA. Due to the cooperative effect of the counterions, part of the chain is saturated with spermine (and its charge close to neutrality) while the other part is still highly negatively charged with no (or low amounts of) condensed spermine. The loose globule is therefore made of a neutral domain (the toroid) and of negatively charged hairs (the coil segment). Kundagrami and Muthukumar (38) reported in other systems how the collection of counterions by the collapsing polymer occurs in tandem with the polymer collapse and how there is a unique mapping between the effective charge and the average coil size. From a biological point of view, DNA chains are always confined in the cell nucleus, and exposed to low amounts of condensing polycations and other condensing agents. These complex conformations of the globule are therefore of the highest interest because the coexistence of neighboring condensed/uncondensed segments

of the chains together with a fine regulation of the inter-distance and nature of the DNA/DNA interactions should provide a fine regulation of the control of the activity of the molecule.

## SUPPLEMENTARY DATA

Supplementary Data are available at NAR Online.

## ACKNOWLEDGEMENT

We thank Marta de Frutos who gave us T5 bacteriophages, M. Renouard who purified the receptor FhuA and Liliane Léger for an interesting discussion on polymer physics.

## FUNDING

French ANR Agency [ANR-12-BSV5-0023-01]; ‘Investissements d’Avenir’ LabEx PALM [ANR-10-LABX-0039-PALM]; Blaise Pascal fellowship (French Government) (to B.S.); Région Ile-de-France (SETCI); Seoul National University (Korea). Funding for open access charge: ANR dotation.

Conflict of interest statement. None declared.

## REFERENCES

- Bloomfield, V.A. (1996) DNA condensation. *Curr. Opin. Struct. Biol.*, **6**, 334–341.
- Post, C.B. and Zimm, B.H. (1982) Theory of DNA condensation: collapse versus aggregation. *Biopolymers*, **21**, 2123–2137.
- Grosberg, A. and Khokhlov, A. (1994) *Statistical Physics of Macromolecules, AIP Series in Polymers and Complex Materials*, American Institute of Physics, NY.
- Post, C.B. and Zimm, B.H. (1982) Light-scattering study of DNA condensation: competition between collapse and aggregation. *Biopolymers*, **21**, 2139–2160.
- Gosule, L.C. and Schellman, J.A. (1976) Compact form of DNA induced by spermidine. *Nature*, **259**, 333–335.
- Chattoraj, D.K., Gosule, L.C. and Schellman, A. (1978) DNA condensation with polyamines. II. Electron microscopic studies. *J. Mol. Biol.*, **121**, 327–337.
- Marx, K.A. and Ruben, G.C. (1983) Evidence for hydrated spermidine calf thymus DNA toruses organized by circumferential DNA wrapping. *Nucleic Acids Res.*, **11**, 1839–1854.
- Hud, N.V. and Downing, K.H. (2001) Cryoelectron microscopy of lambda phage DNA condensates in vitreous ice: the fine structure of DNA toroids. *Proc. Natl. Acad. Sci. U.S.A.*, **98**, 14925–14930.
- Widom, J. and Baldwin, R.L. (1983) Monomolecular condensation of lambda-DNA induced by cobalt hexammine. *Biopolymers*, **22**, 1595–1620.
- Jary, D. (1998) *Etude des propriétés statiques et dynamiques de longues chaînes d’ADN sur deux exemples : rhéologie de solutions semi-diluées et cyclisation d’une chaîne globulaire*. Ph.D. Thesis, Orsay University, France.
- Jary, D. and Sikorav, J.L. (1999) Cyclization of globular DNA. Implications for DNA-DNA interactions in vivo. *Biochemistry*, **38**, 3223–3227.
- Minagawa, K., Matsuzawa, Y., Yoshikawa, K., Matsumoto, M. and Doi, M. (1991) Direct observation of the biphasic conformational change of DNA induced by cationic polymers. *FEBS Lett.*, **295**, 67–69.
- Ueda, M. and Yoshikawa, K. (1996) Phase transition and phase segregation in a single double-stranded DNA molecule. *Phys. Rev. Lett.*, **77**, 2133–2136.
- Hsu, H.P. and Grassberger, P. (2005) The coil-globule transition of confined polymers. *J. Stat. Mech. Theory Exp.*, P01007.
- Hsu, H.-P., Paul, W. and Binder, K. (2006) Intramolecular phase separation of copolymer “bottle brushes”: No sharp phase transition but a tunable length scale. *Europhys. Lett.*, **76**, 526–532.
- Leforestier, A. and Livolant, F. (2009) Structure of toroidal DNA collapsed inside the phage capsid. *Proc. Natl. Acad. Sci. U.S.A.*, **106**, 9157–9162.
- Leforestier, A., Brasiles, S., de Frutos, M., Raspaud, E., Letellier, L., Tavares, P. and Livolant, F. (2008) Bacteriophage T5 DNA Ejection under Pressure. *J. Mol. Biol.*, **384**, 730–739.
- Boulanger, P., leMaire, M., Bonhivers, M., Dubois, S., Desmadril, M. and Letellier, L. (1996) Purification and structural and functional characterization of FhuA, a transporter of the Escherichia coli outer membrane. *Biochemistry*, **35**, 14216–14224.
- Leforestier, A. and Livolant, F. (2010) The bacteriophage genome undergoes a succession of intracapsid phase transitions upon DNA ejection. *J. Mol. Biol.*, **396**, 384–395.
- Tzili, S., Kindt, J. T., Gelbart, W.M. and Ben-Shaul, A. (2003) Forces and pressures in DNA packaging and release from viral capsids. *Biophys. J.*, **84**, 1616–1627.
- Gosule, L.C. and Schellman, J.A. (1978) DNA condensation with polyamines I. Spectroscopic studies. *J. Mol. Biol.*, **121**, 311–326.
- Melnikov, S.M., Sergeyev, V.G. and Yoshikawa, K. (1995) Discrete coil-globule transition of large DNA induced by cationic surfactant. *J. Am. Chem. Soc.*, **117**, 2401–2408.
- Yamasaki, Y., Katayose, S., Kataoka, K. and Yoshikawa, K. (2003) PEG-PLL block copolymers induce reversible large discrete coil-globule transition in a single DNA molecule through cooperative complex formation. *Macromolecules*, **36**, 6276–6279.
- Takahashi, M., Yoshikawa, K., Vasilevskaya, V.V. and Khokhlov, A.R. (1997) Discrete coil-globule transition of single duplex DNAs induced by polyamines. *J. Phys. Chem. B*, **101**, 9396–9401.
- Evilevitch, A., Gober, J.W., Phillips, M., Knobler, C.M. and Gelbart, W.M. (2005) Measurements of DNA lengths remaining in a viral capsid after osmotically suppressed partial ejection. *Biophys. J.*, **88**, 751–756.
- Raspaud, E., Durand, D. and Livolant, F. (2005) Interhelical spacing in liquid crystalline spermine and spermidine-DNA precipitates. *Biophys. J.*, **88**, 392–403.
- Todd, B.A., Parsegian, V.A., Shirahata, A., Thomas, T.J. and Rau, D.C. (2008) Attractive forces between cation condensed DNA double helices. *Biophys. J.*, **94**, 4775–4782.
- Iwaki, T., Makita, N. and Yoshikawa, K. (2008) Folding transition of a single semiflexible polyelectrolyte chain through toroidal bundling of loop structures. *J. Chem. Phys.*, **129**, 065103.
- Brewer, L.R., Corzett, M. and Balhorn, R. (1999) Protamine-induced condensation and decondensation of the same DNA molecule. *Science*, **286**, 120–123.
- Miyazawa, N., Sakaue, T., Yoshikawa, K. and Zana, R. (2005) Rings-on-a-string chain structure in DNA. *J. Chem. Phys.*, **122**, 044902.
- Odijk, T. (2008) Scaling theory of DNA confined in nanochannels and nanoslits. *Phys. Rev. E*, **77**, 060901.
- Sakaue, T. (2007) Semiflexible polymer confined in closed spaces. *Macromolecules*, **40**, 5206–5211.
- Marenz, M., Zierenberg, J., Arkin, H. and Janke, W. (2012) Simple flexible polymers in a spherical cage. *Condens. Matter Phys.*, **15**, UNSP 43008.
- Oskolkov, N.N., Linse, P., Potemkin, I.I. and Khokhlov, A.R. (2011) Nematic ordering of polymers in confined geometry applied to DNA packaging in viral capsids. *J. Phys. Chem. B*, **115**, 422–432.
- Cacciuto, A. and Luijten, E. (2006) Self-avoiding flexible polymers under spherical confinement. *Nano Lett.*, **6**, 901–905.
- Smyda, M.R. and Harvey, S.C. (2012) The entropic cost of polymer confinement. *J. Phys. Chem. B*, **116**, 10928–10934.
- Sakaue, T. and Raphael, E. (2006) Polymer chains in confined spaces and flow-injection problems: Some remarks. *Macromolecules*, **39**, 2621–2628.
- Kundagrami, A. and Muthukumar, M. (2010) Effective charge and coll-globule transition of a polyelectrolyte chain. *Macromolecules*, **43**, 2574–2581.